Electrochimica Acta 53 (2008) 5819–5826

Contents lists available at ScienceDirect

Electrochimica Acta

journal homepage: www.elsevier.com/locate/electacta

Estimation of ion-site association constants in ion-selective electrode membranes by modified segmented sandwich membrane method

Maria A. Peshkova, Anton I. Korobeynikov, Konstantin N. Mikhelson*,[1]

St. Petersburg State University, St. Petersburg, Russia

ARTICLE INFO

Article history:
Received 5 January 2008
Received in revised form 21 February 2008
Accepted 13 March 2008
Available online 21 March 2008

Keywords:
Ion-site association constants
Ion-selective electrodes
Segmented sandwich membranes

ABSTRACT

A method aimed at potentiometric estimation of the association of ions with ion-exchanger sites and charged ionophores in ion-selective electrode membranes is proposed. The method relies on the measurements of segmented sandwich membrane potentials. It is shown theoretically that the quantification of ion association requires use of weakly associated ionic additive whose concentration in the working segment of the sandwich must be varied. This is in contrast with well-established technique of ion to neutral ionophore complexation measurements. The advantages and limitations of the novel method are critically evaluated. Association of ions in plasticized poly(vinylchloride) membranes is studied experimentally. Experimental results are provided related to the association of K^+, Na^+, Cs^+, and NH_4^+, and also Ca^{2+} with commonly used sites: tetra(*p*-Cl-phenyl)borate anion and calcium-selective lipophilic ion-exchanger bis[4-(1,1,3,3-tetramethylbutyl)phenyl]phosphate.

1. Introduction

Ion-selective electrodes (ISEs) with membranes containing ionophores constitute one of the most important kinds of electrochemical sensors [1,2]. Selectivity of ISEs, together with the detection limit, is the most crucial characteristics of these sensors. It was shown in recent years, both experimentally [3–5] and theoretically [6–9] that the selectivity and the detection limit, if properly measured, are inseparably linked to one another. Therefore, detailed knowledge of the species interactions in real membranes which is obviously needed for understanding of the selectivity is also needed for better insight of the ultimate limits of the ISE response.

For decades, it was recognized that the selectivity of ISEs with neutral ionophores is governed, primarily, by complexation of ions with the ionophore in the membrane [10,11]. The association between ions and ion-exchanger sites in membranes was considered as minor effect, and often neglected in theoretical considerations [11], and this was in good agreement with numerous experimental results. On the other hand, already in early years of ISE theory and practice, it was shown that the impact of ion-site association to selectivity can be crucial [10,12]. Basically, there are three reasons for this apparent paradox. In the first place, the selectivity of association does not fully manifest in the potentiometric selectivity of ISEs. For instance, for monovalent ions, selectivity coefficient is proportional to square root of the ratio of association constants of J^+ interference ion and I^+ target analyte with R^- sites: $K_{IJ} \sim \sqrt{K_{JR}/K_{IR}}$ [13,14]. On the contrary, the selectivity of ion complexation with L neutral ionophore displays in the potentiometric selectivity in "full scale" and the selectivity coefficient is directly proportional to the ratio of the respective complex formation constants: $K_{IJ} \sim K_{JL}/K_{IL}$ [10,11,14]. In the formulas above K_{IJ} stands for the potentiometric selectivity coefficient to I^+ over J^+ ions, K_{JR} and K_{IR} are association constants of J^+ and I^+ with R^- sites, while K_{JL} and K_{IL} denote formation constants of JL^+ and IL^+ complexes.

The second reason is the screening effect of a bulky neutral ionophore over ion within the complex, so that the specific nature of the ion cannot be accessed by the sites. This effect results in similar affinity of sites to all complexed ions: target analyte and interferences.

The third reason why ion-site association did not appear relevant was historical. First lipophilic ionic sites used in ISE membranes were substituted tetraphenylborates or quaternary ammonium ions. These sites hardly provide high selectivity of association. Rare examples of selective sites which nowadays are called charged ionophores were alkylphosphoric acids used as sites in calcium-selective membranes [15,16].

This is why studies of ion-site association constants did not attract so much effort as similar studies of complexation of ions by neutral ionophores. Therefore, even after decades of develop-

* Corresponding author. Tel.: +7 812 428 4103; fax: +7 812 428 6939.
E-mail address: konst@km3241.spb.edu (K.N. Mikhelson).
[1] ISE member.

0013-4686/$ – see front matter © 2008 Elsevier Ltd. All rights reserved.
doi:10.1016/j.electacta.2008.03.030

ment and application of ISEs there is almost no data on the values of association constants in real electrode membranes.

On the other hand, these data became nowadays highly relevant. A number of various charged ionophores (e.g., porphyrines, salophenes) are now available, and these charged ionophores bind ions selectively [17]. Also, it was shown that by means of ionic additives (lipophilic ions charged oppositely to the main sites) it is possible to take full advantage of selective ion-site association, so that the potentiometric selectivity coefficient is directly proportional to the ratio of ion-site association constants [13,14]. Computer simulations performed in [18] showed that in the case of highly selective ion-site association one could anticipate significant impact of this effect to overall selectivity of membranes. Unfortunately, quantification of ion-site association in real membranes is a difficult challenge. Use of optical methods is hampered by absorbance of the membrane solvent (plasticizer) and also of PVC. Conductivity of membranes can be easily measured, but conductivity relates to the flux of moving species, and therefore, delivers the multiple of the concentration of dissociated ions, and their mobility. Proper separation of the multiple into concentration factor and mobility factor is not trivial [19].

In principle, species interactions in real membranes can be accessed by segmented sandwich membrane method. This method has been invented first in [20] and was successfully used for quantification of complexation of ions by neutral ionophores [21–26]. However, as it was demonstrated in [23], the same approach does not allow for measurements of ion-site association constants. It is only possible to distinguish between strong and weak association, and it was shown that even tetraphenylborate salts are strongly associated in ISE membranes [23]. A modification of segmented sandwich membrane method which, in principle, may allow for direct measurements of ion-site association constants in real membranes was briefly discussed for the first time in [18].

In this paper we will describe the theory of this modified method in more detail, discussing also the limitations of the proposed technique. Experimental results will be provided, related to the association of monovalent cations and calcium with commonly used sites: tetra(*p*-Cl-phenyl) borate and calcium-selective ion-exchanger bis[4-(1,1,3,3-tetramethylbutyl)phenyl]phosphate.

2. Theory

The theory of the method relies on multispecies approach (MSA) described earlier [21,27–29]. Essentially, MSA considers a number of species for each ion which is present in the membrane. These are: the free ion, a number of complexes of the ion with a neutral ionophore (with different stoichiometric composition), and the respective ion pairs and triplets with the ion-exchanger and charged ionophore, if applicable. This is in contrast with some other approaches dealing with only one particular kind of species for each ion in the membrane, for instance only one sort of complexes, no association, etc. Therefore, MSA is advantageous for the continuous description of membranes with broad variation of the concentrations of ionophores and sites. This approach only deals with a quasi-steady state, like well-known descriptions summarized in [10,11]. The latter, however, refer only to relatively simple, idealized cases, mostly—when association of ions in membranes is neglected. The MSA, on the contrary, allows for the consideration of membrane potentials, including segmented sandwich membrane potential, with any degree of association of the electrolyte in the membrane. Since segmented sandwich membrane potential is essentially time-dependent, more advanced, high level description based on solution of Nernst–Plank and Poisson equations in real space and time (NPP model) [7–9] would be useful here. However, to the best of our knowledge, the NPP model does not consider association effects in membranes, at least at the current stage of development. This is why here we will take advantage of numerical modeling in the framework of MSA.

To clarify the difference between the two modifications of the segmented sandwich membrane method: that (i) aimed at measuring complexation by neutral ionophore, and that (ii) aimed at quantification of ion-site association, we will briefly remind the basics of modification (i).

The main idea of the method is making the concentration of the ionophore different on the two opposite sides of the membrane. In such a case, the impacts to the chemical potential of the ion related to the interaction with the neutral ionophore on the two sides do not eliminate one another, so that the overall membrane potential in otherwise symmetric cell is a measure of the ion-to-ionophore complexation.

To implement this idea, the membrane consists of two segments, which are fused immediately before measurements. The composition of one of the segments (reference segment) is kept constant. The composition of the other segment (working segment) is the same as that of the reference segment, except of C_L^{tot} the total concentration of the ionophore, and the latter is varied. When the neutral ionophore is in excess over sites the electric potential of the segmented sandwich membrane follows simple equation:

$$E = n\frac{RT}{F}\ln C_L^{tot} + \frac{RT}{F}\ln K_{ILn} \quad (1)$$

Here, K_{ILn} stands for stability constant of complex IL_n^+. Basically, measurements of complex stability constants by segmented sandwich membrane method rely on this equation. In more details, the method is described in [23,25].

As shown in [23] this particular approach: when the content of the ionophore of interest is varied in the working segment, does not allow for measurements of ion-site association constant. Simulation by means of MSA gives further insight to this issue. Example of simulated segmented sandwich membrane potential, when C_R^{tot} total concentration of R^- is varied in the working segment is presented in Fig. 1. The simulations have been performed using the system of equations very similar to published in [18]. Only boundary potentials were considered, being expressed in terms of a_I activity of I^{z+} potential determining ions in aqueous solution, and

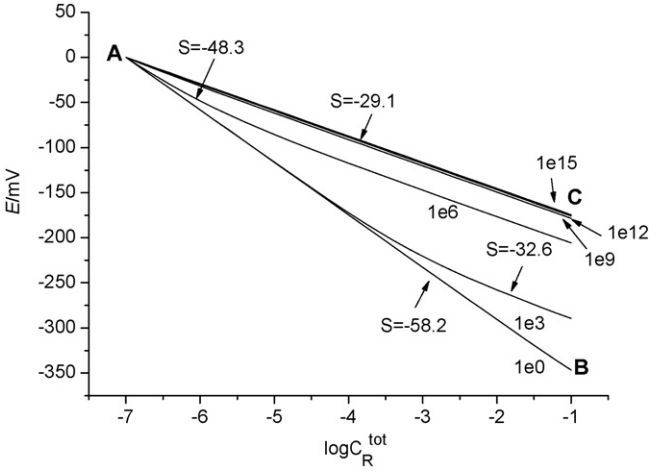

Fig. 1. Simulated curves of segmented sandwich membrane potential for different values of K_{IR} (from 1 to 10^{15} M^{-1}) when C_R^{tot} total concentration of sites is varied in the working segment. In the reference segment, $C_R^{tot} = 10^{-7}$ M.

C_I concentration of these free ions in the membrane:

$$E_b = E^{mem} - E^{aq} = -\frac{\mu_I^{0,mem} - \mu_I^{0,aq}}{z_I F} + \frac{RT}{z_I F} \ln \frac{a_I}{C_I} \quad (2)$$

Here μ_I^0 stand for standard values of the chemical potential of I^{z+} in the membrane and in the aqueous phase, denoted, respectively, with superscripts mem or aq. The standard values of the chemical potentials of I^{z+} are the same in both segments because of the same PVC and the same plasticizer. The compositions of aqueous solutions on both sides of the sandwich are also the same. The impact from the diffusion potential at the junction between the two segments is neglected here. Under these conditions the overall electric potential of the sandwich membrane can be written as follows:

$$E = E_b^{work} + E_b^{ref} = \frac{RT}{z_I F} \ln \frac{C_I^{ref}}{C_I^{work}} \quad (3)$$

Concentration of I^{z+} free ions for given values of C_R^{tot} and C_S^{tot} (total concentration of S^+ ionic additive, if applicable) and given values for the respective association constants can be accessed by solving the system of material and charge balance equations below:

$$C_R^{tot} = C_R + \sum_{q=1}^{z} q C_{IR_q} + C_{SR} \quad (4)$$

$$C_S^{tot} = C_S + C_{SR} \quad (5)$$

$$C_R = \sum_{q=0}^{z} (z-q) C_{IR_q} + C_S \quad (6)$$

The system of Eqs. (4)–(6) can be solved using objective function method. A suitable objective function combines disbalances of the concentrations of the membrane components:

$$\Phi = \left(\frac{C_R^{tot} - C_R^{comb} - C_R}{C_R} \right)^2 + \left(\frac{C_S^{tot} - C_S^{comb} - C_S}{C_S} \right)^2 \quad (7)$$

Superscript comb denotes sums of the concentrations of all species which include the component, except of the respective free species. The true values of all the species concentrations return zero value of the objective function.

The values of K_{IR} association constant in these simulations were 1, 10^3, 10^6, 10^9, 10^{12} and 10^{15} M^{-1}, and C_R^{tot} in the reference segment was 10^{-7} M. The latter value is unrealistically small for real membranes, but chosen here for purpose: it allows for demonstration of Nernstian and half-Nernstian slopes in different domains of the same curve if the association constant is relatively low. The curve obtained for $K_{IR} = 1$ M^{-1} is linear with Nernstian slope −58.1 mV. The curves calculated for $K_{IR} = 10^9$ M^{-1} and higher show half-Nernstian slope of −28.2 mV, and these curves practically coincide. In the curve related to the $K_{IR} = 10^3$ M^{-1} one can see two well-resolved domains, with Nernstian slope at $C_R^{tot} < 10^{-4}$ M, and half-Nernstian slope at $C_R^{tot} > 10^{-3}$ M. The curve calculated for $K_{IR} = 10^6$ M^{-1} contains a small domain with sub-Nernstian slope of 48.3 mV when $C_R^{tot} < 10^{-6}$ M, and in the rest of the curve the slope is half-Nernstian. These results are consistent with earlier data [23].

The results can be easily rationalized for limited cases of full dissociation and of strong association. Here we will take advantage of the conditions of bulk electroneutrality: $C_I = C_R$, that of material balance for R^- sites: $C_R^{tot} = C_R + C_{IR}$, and of the mass law for the association constant: $C_{IR} = C_I C_R K_{IR}$.

Bearing these conditions in mind, we immediately obtain for the limiting case of full dissociation

$$C_I = C_R \approx C_R^{tot} \quad (8)$$

while for the limiting case of strong association

$$C_I \approx \sqrt{C_R^{tot}/K_{IR}} \quad (9)$$

Thus C_I always increases with increasing C_R^{tot} producing negative slope of the EMF curve, and the slope varies between Nernstian in the case of full dissociation, and half-Nernstian for strong association.

At high values of K_{IR} the concentration of free I^+ ions is inversely proportional to the square root of K_{IR}, see Eq. (9). However, the EMF curves not always show this dependence, and tend to come close to one another, or even coincide with increasing K_{IR}. This is because all the curves start from the same point with $E = 0$ (point A in Fig. 1) when the compositions of the working segment and the reference segment are the same. So, at high association, Eq. (9) is fulfilled for both segments, effectively eliminating the impact from the value of K_{IR}.

The shape of the curves plotted in Fig. 1 depends on whether the membranes refer to only one of the aforementioned limiting cases, within the whole range of variation of C_R^{tot}, or full dissociation at low values of C_R^{tot} is followed by strong association at high C_R^{tot}. On the whole, higher values of association constant give lower effects in the EMF. Anyway, any response curve is expected to be located between lines AB – for dissociated membranes, and AC – for associated membranes. One can conclude, therefore, that this particular setup is hardly suitable for quantification of ion-site interactions in ISE membranes.

On the other hand, computer simulations by means of MSA, implemented in the same way as above, allowed us to reveal another experimental setup, and now it will be demonstrated that this modified setup is promising in view of quantification of ion-site association in the real membranes. The essence of the modified setup is that the total concentration of sites in the working segment must be constant, and be the same as in the reference segment. However, the working segment must contain lipophilic ionic additive (co-exchanger) charged oppositely to the sites, and the concentration of the additive must be varied.

The results of MSA simulations of segmented sandwich membrane potentials and concentrations of individual species are presented in Fig. 2A and B. The simulations were performed for membranes with the same set of the values of K_{IR} association constants as shown in Fig. 1. Interaction between S^+ additive and R^- sites was assumed rather weak: $K_{SR} = 1$. This assumption may be realistic for bulky S^+ additive and R^- sites with low density of charge.

One can see that according to the MSA modeling, variation of the concentration of the ionic additive allows obtaining EMF response, increasing with the increase of the content of the additive, and also with the increase of the association constant. At relatively high values of K_{IR}, like 10^6 M^{-1} the simulated curves contain linear domain with Nernstian slope. When the values of association constants are even higher, $K_{IR} \geq 10^{12}$ M^{-1} the simulated curves tend to come close to one another, and the whole response curve is Nernstian.

For rationalization of the shape of the EMF curves presented in Fig. 2A, we will turn now to the curves of the individual species concentrations. The selection of the respective curves are presented in Fig. 2B. Comparison of the EMF curves (Fig. 2A) and the species concentration curves (Fig. 2B) for strong association ($K_{IR} = 10^6$, 10^9, and 10^{12} M^{-1}) allows concluding the following. The initial flat part of the response curve, when the concentration of the additive is low, refers to the conditions: $C_{IR} \approx C_R^{tot}$, and $C_I \approx C_R$. Thus, in the initial horizontal part of the curve:

$$C_I \approx \left(\frac{C_R^{tot}}{K_{IR}} \right)^{1/2} \quad (10)$$

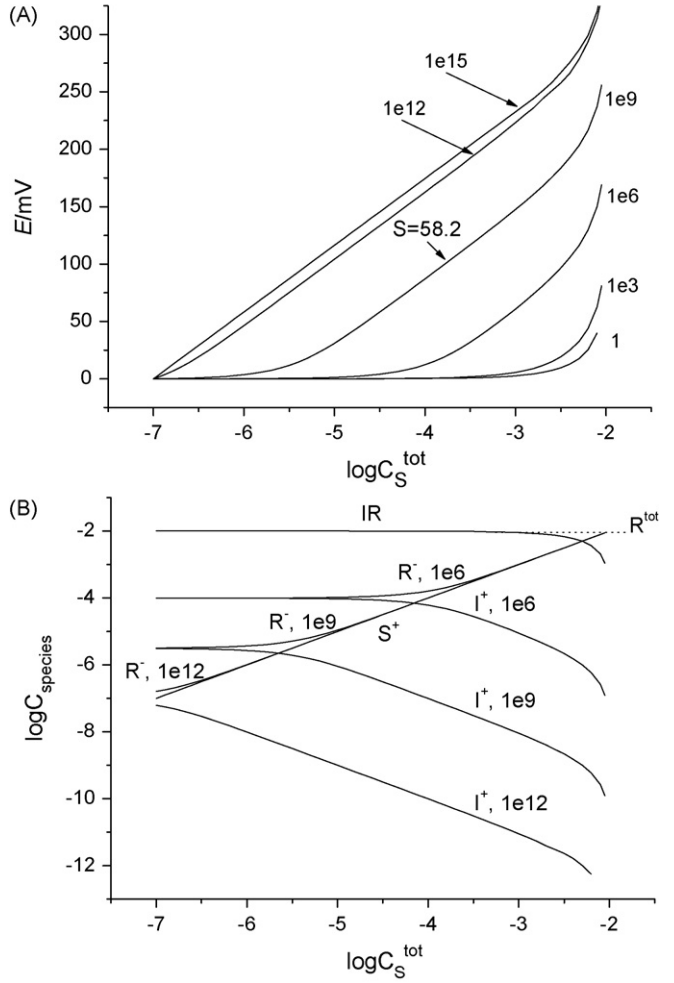

Fig. 2. Simulated curves of segmented sandwich membrane potential (A) and individual species concentrations in the working segment (B), for membranes with K_{IR} within the range from 1 through 10^{15} M^{-1}. In the reference segment, $C_S^{tot} = 10^{-7}$ M, in the working segment C_S^{tot} is varied. Total concentration of R^- sites is constant in both segments, $C_R^{tot} = 10^{-2}$ M.

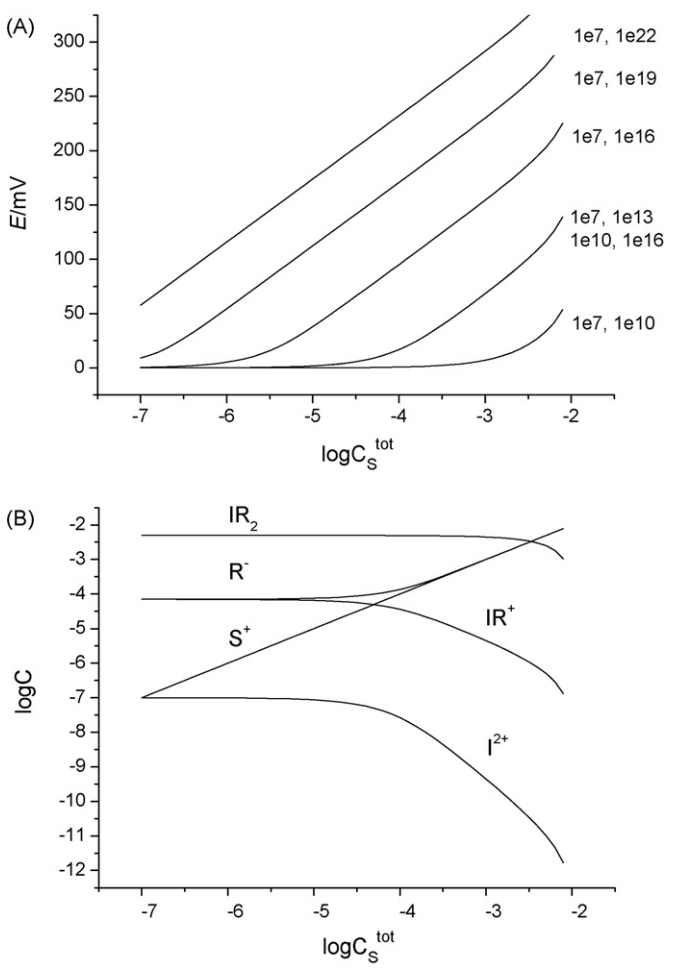

Fig. 3. Simulated curves of segmented sandwich membrane potential (A), and of the concentrations of the individual species in working segment (B), when C_S^{tot} is varied in the working segment. In the reference segment, $C_S^{tot} = 10^{-7}$ M. The total concentration of R^- sites is constant in both segments, $C_R^{tot} = 10^{-2}$ M. In (A) $K_{IR} = 10^7$ M^{-1} (or 10^{10} M^{-1}), $\beta_{IRR} = 10^{10}$, 10^{13}, 10^{16}, and 10^{22} M^{-2} (or 10^{16} M^{-2}). In (B) $K_{IR} = 10^7$ M^{-1}, $\beta_{IRR} = 10^{13}$ M^{-2}.

Eq. (10) holds also for the reference segment since it does not contain the additive. The linear domain in the response curves shown in Fig. 2 refers to the conditions: $C_{IR} \approx C_R^{tot}$, and $C_R \approx C_S \approx C_S^{tot}$. Thus, in the linear domain:

$$C_I \approx \frac{C_R^{tot}}{C_S^{tot} K_{IR}} \tag{11}$$

Considering only boundary potentials, we can obtain for the overall sandwich membrane potential in the linear domain:

$$E = \frac{RT}{F} \ln \frac{C_I^{ref}}{C_I^{work}} = \frac{RT}{F} \left(\frac{1}{2} \ln K_{IR} + \ln C_S^{tot} - \frac{1}{2} \ln C_R^{tot} \right) \tag{12}$$

Thus, the modified setup for the segmented sandwich membrane method allows for measurement of the ion-site association constants in real membranes.

This simple behavior can be anticipated only for membranes with strong ion-site association and weak interaction between the main sites and lipophilic additive. Otherwise one cannot expect linear domains in the curves of segmented sandwich membrane potential. Interpretation of experimental results obtained for membranes with $K_{IR} < 10^6$ M^{-1}, or with commensurable values of K_{IR} and K_{SR} may require nonlinear fitting of the data.

Simulated EMF curves presented in Fig. 2A tend to coincide at very high association constants, so the EMF is not more sensitive to the value of K_{IR}. This trend can be clarified with the data presented in Fig. 2B. If IR associates too strongly, the condition $C_I \approx C_R$ does not hold even at very low concentrations of S^+ additive, so essentially $C_R \approx C_S \approx C_S^{tot}$ is valid in the whole range of C_S^{tot}. Decrease of C_S^{tot} down to zero is possible in simulations, but hardly possible in real membranes because of inevitable impurities. Thus, the proposed method is limited to membranes with moderate values of ion-site association constants.

We will turn now to the case of the association of divalent ions with monovalent sites. Using the same approach as for monovalent ions, we can envisage the following regularities for segmented sandwich membranes with variation of S^+ monovalent additive and constant total content of R^- sites.

The simulated EMF curves for membranes with first association constant $K_{IR} = 10^7$ M^{-1}, and the cumulative association constant β_{IRR} within the range from 10^{10} through 10^{16} M^{-2} are presented in Fig. 3A. The respective curves for the concentrations of the individual species for membrane with $K_{IR} = 10^7$ M^{-1}, $\beta_{IRR} = 10^{13}$ M^{-2} are given in Fig. 3B. The results demonstrate the possibility to measure the ratio between β_{IRR} and K_{IR}, as we will show below.

As one can see from Fig. 3B, in the initial horizontal part of the curve, and in the reference segment (with low concentration of S^+ additive) $C_{IRR} \approx C_R^{tot}/2$, and $C_{IR} \approx C_R$. Therefore, in the reference segment $C_I K_{IR} = 1$, and

$$C_I = K_{IR}^{-1} \quad (13)$$

As to the working segment, in the linear part of the response curve (compare Fig. 3A and B) $C_{IRR} \approx C_R^{tot}/2$, and $C_R \approx C_S \approx C_S^{tot}$. Thus, in the working segment

$$C_I = \frac{C_R^{tot}/2}{(C_S^{tot})^2 \beta_{IRR}} \quad (14)$$

Considering only boundary potentials, we can obtain for the overall sandwich membrane potential in the linear domain:

$$E = \frac{RT}{2F} \ln \frac{C_I^{ref}}{C_I^{work}} = \frac{RT}{2F} \left(\ln \left(\frac{\beta_{IRR}}{K_{IR}} \right) + 2 \ln C_S^{tot} - \ln \left(\frac{C_R^{tot}}{2} \right) \right) \quad (15)$$

As predicted by Eq. (15), only the ratio of the cumulative association constant over the first step constant can be accessed. More of this, the whole curves (not only linear domains) for $K_{IR} = 10^7\ M^{-1}$, $\beta_{IRR} = 10^{13}\ M^{-2}$ and for $K_{IR} = 10^{10}\ M^{-1}$, $\beta_{IRR} = 10^{16}\ M^{-2}$ coincide.

The considerations presented above and in particular Eqs. (12) and (15) show the possibility of assessing association constants of ions and sites or charged ionophores in real ISE membranes by measurements of segmented sandwich membrane potentials with variation of ionic additive in the working segment. Unfortunately, for the association between divalent ions and monovalent sites or charged ionophores only the ratio of the cumulative association constant over the first step association constant can be assessed by this method. In addition, diffusion potential in the vicinity of the segment junction (neglected in the theory above) may produce some uncertainty about the values obtained.

3. Experimental

Potassium tetrakis-*p*-Cl-phenylborate (KClTPB), tetradodecylammonium tetrakis-*p*-Cl-phenylborate (ETH 500), and solvent plasticizers bis(butylpentyl)adipate (BBPA) and *o*-nitrophenyloctyl ether (oNPOE) were Selectophore grade reagents from Fluka (Buchs, Switzerland). Ca^{2+}-selective ion-exchanger bis[4-(1,1,3,3-tetramethylbutyl)phenyl]phosphate ($TMBPP^-$) and Ca^{2+}-membrane plasticizer bis(dioctylphenyl)phosphonate (DOPP), both of the highest purity available, were generous gifts from Radiometer (Copenhagen, Denmark). Tetradecylammonium bromide (TDABr) was from Analyse-X (Minsk, Belarus). High molecular weight Poly(vinylchloride) S-66 (PVC) was from Ohtalen (St. Petersburg, Russia). Volatile solvents were extra pure cyclohexanone (CH) from Vekton, St. Petersburg, Russia, and HPLC grade tetrahydrofuran (THF) from Vekton, St. Petersburg, Russia. Analytical grade inorganic electrolytes: KCl, NaCl, CsCl, NH_4Cl, and $CaCl_2$ were from Reachim (Moscow, Russia). All aqueous solutions were prepared with distilled or bidistilled water.

Membrane cocktails were prepared by mixing appropriate amounts of PVC and the respective plasticizer (the mass ratio was always 1:2), and dissolving them in freshly distilled THF. After that the respective ion-exchanger and (if applicable) also ETH 500 were added as appropriate aliquots of stock solutions in CH. In this way taking small weights was avoided, and high accuracy of membrane compositions was ensured. The dry content in the cocktails was 13–14%. The total concentration of the cation-exchanger sites (C_R^{tot}) was the same both in the working and in the reference segment. For KClTPB it was always 0.01 m, and for $CaTMBPP_2$ it was 0.02 m. Cocktails for reference segments did not contain additive. The total concentration of the additive (C_S^{tot}) in membranes to constitute working segments varied from 10 to 90% (molar) of C_R^{tot}. The appropriate total concentrations of the cation-exchanger sites (C_R^{tot}) and that of the total additive (C_S^{tot}) were set by adding of suitable quantities of KClTPB and ETH 500 to the cocktails. Direct adding of quaternary ammonium salts, e.g., as bromides or chlorides instead of ETH 500, is not recommended because inorganic salt (e.g., KBr) which forms in the membrane tends to remain there for several days of soaking. The presence of an inorganic salt in the membrane becomes apparent when membrane is dried after being in contact with water. The inorganic salt (if present) accumulates in water droplets within the membrane, and forms tiny but visible pieces of salt upon drying. On the other hand, proper mixture of KClTPB and ETH 500 ensures the required ratio of R^- over S^+, and the only inorganic ion in the membrane is K^+. In the case of Ca^{2+}-membranes this technique was not possible, and tetradecylammonium was added as bromide salt (TDABr). Therefore, calcium membranes were soaked in aqueous solutions until fully transparent when after contact with water.

To obtain membranes, the cocktails were sonicated for 10 min and then casted on glass Petri dishes and closed with filter paper to slow down the evaporation of THF. The electrodes for potentiometric measurements were prepared by cutting disks with diameter of 12 mm from thick (0.7 mm) master membranes and gluing them to PVC bodies with outer diameter of 12 mm and inner diameter of 10 mm. A solution of PVC in CH was used as the glue. Membranes for chronopotentiometric measurements were much thinner: 65–80 μm, while the outer diameter of the bodies for chronopotentiometry was 16 mm, and the inner diameter was 15 mm. This geometry was chosen for reliable recording of the polarization in the vicinity of membrane/solution surface in spite of high Ohmic resistance of the membrane bulk.

Before measurements the electrodes were filled with 0.01 M solution of the respective chloride salt, and conditioned in the same solution. The conditioning time was 2–3 days for K^+ and 3–5 days for Ca^{2+}. To convert KClTPB initially present in membranes into the respective Na^+, Cs^+, or NH_4^+ salt, the conditioning time was 2 weeks.

Potentiometric measurements were performed with pX/mV-meter pX-150 and saturated Ag/AgCl reference electrode, both from Izmeritel, Gomel, Belarus. The reference electrode was connected to the calibrator solution with 3.5 M KCl salt bridge with limited diffusion, so that the contamination of the calibrator solution with KCl was negligible. The internal electrode was always Ag/AgCl. The calibrators were pure aqueous solutions of the respective chloride salts, within the concentration range 10^{-5} to 0.1 M. The electrodes which showed Nernstian response were used for further research by segmented sandwich membrane method. For these measurements the electrodes with membranes of different compositions were pressed membrane-to-membrane and fixed mechanically, so that two membranes were fused into sandwich, and the EMF was recorded by connection of the meter to two internal Ag/AgCl electrodes.

Chronopotentiometric measurements were performed for totally symmetric cells: the same electrolyte of the same concentration was used in the inner and outer solutions. Chlorinated silver wire electrodes (working and reference), and glassy carbon counter electrode were used. The chronopotentiometric curves were recorded with Autolab PGstat 20 (Eco Chemie, The Netherlands). The current was zero for first 10 s, followed with pulse of 10^{-7} A for 100 s, and then again zero current for 10 s.

All the measurements were carried out at room temperature (23 ± 2 °C), with 3 replica electrodes for statistics.

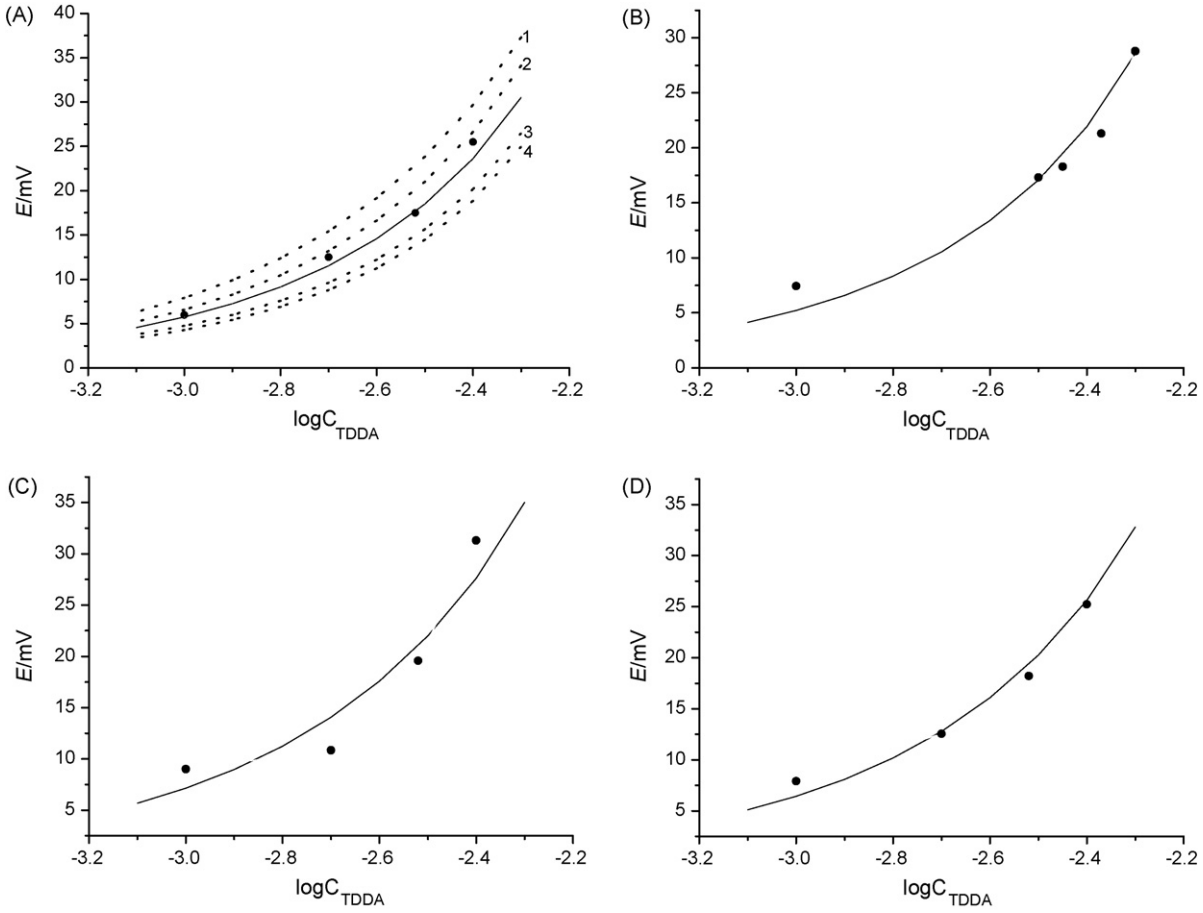

Fig. 4. Potentials of segmented sandwich membranes plasticized with BBPA, equilibrated with KCl (A), NaCl (B), CsCl (C), and NH_4Cl (D). Dots refer to the experimental data, and solid curves to the data calculated with $K_{KClTPB} = 2.5 \times 10^3\ M^{-1}$, $K_{NaClTPB} = 2.0 \times 10^3\ M^{-1}$, $K_{CsClTPB} = 4.0 \times 10^3\ M^{-1}$, $K_{NH4ClTPB} = 3.2 \times 10^3\ M^{-1}$, and $K_{TDDAClTPB} = 2.5 \times 10^2\ M^{-1}$. Dotted curves in A refer to $K_{KClTPB} = 5.0 \times 10^3\ M^{-1}$, $K_{TDDAClTPB} = 2.5 \times 10^2\ M^{-1}$ (curve 1); $K_{KClTPB} = 2.5 \times 10^3\ M^{-1}$, $K_{TDDAClTPB} = 1.25 \times 10^2\ M^{-1}$ (curve 2); $K_{KClTPB} = 2.5 \times 10^3\ M^{-1}$, $K_{TDDAClTPB} = 5 \times 10^2\ M^{-1}$ (curve 3); $K_{KClTPB} = 1.25 \times 10^3\ M^{-1}$, $K_{TDDAClTPB} = 2.5 \times 10^2\ M^{-1}$ (curve 4).

4. Results and discussion

4.1. Membranes containing tetrakis(p-Cl-phenyl)borate

To study ion-pairing between monovalent cations and tetrakis(*p*-Cl-phenyl)borate anion in membranes of different polarities, 2 series of membranes were prepared: plasticized with BBPA, and with oNPOE. Each membrane contained constant total concentration of tetrakis(*p*-Cl-phenyl)borate, while the concentration of lipophilic cation: tetradodecylammonium ($TDDA^+$) varied from 0 to 90% (mol/mol) relative to tetrakis(*p*-Cl-phenyl)borate.

Electrodes with BBPA membranes containing up to 42% (mol) of $TDDA^+$ relative to $ClTPB^-$ showed Nernstian cationic slope ($S = 57–58$ mV) in solutions of KCl, NaCl, CsCl, and NH_4Cl, in concentration range 10^{-5} to 10^{-1} M. However, electrodes with higher content of the $TDDA^+$ additive showed sub-Nernstian slope or no slope at all. In the case of oNPOE as plasticizer, Nernstian cationic slope was obtained from electrodes with membranes containing up to 75% (mol) of $TDDA^+$. The values of the segmented sandwich membrane potentials for membranes providing zero slope achieved 300 mV, and to some extent refer to ion distribution coefficients [30]. Below, we will consider only the data obtained from membranes providing full Nernstian cationic response.

The reference segment membranes contained 0.01 M KClTPB without $TDDA^+$, and showed full Nernstian cationic response. Ion pairing of tetrakis(*p*-Cl-phenyl)borate anion in BBPA was studied for monovalent cations: K^+, Na^+, Cs^+, and NH_4^+. The results are presented in Fig. 4A–D. In the case of oNPOE only K^+ was studied, and the results are presented in Fig. 5.

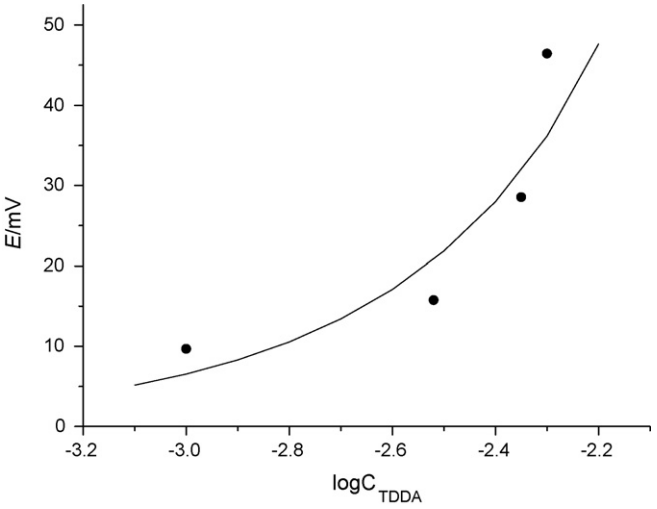

Fig. 5. Potentials of segmented sandwich membranes plasticized with oNPOE, equilibrated with KCl. Dots refer to the experimental data, and curve to the data calculated with $K_{KClTPB} = 1.6 \times 10^3\ M^{-1}$, $K_{TDDAClTPB} = 10\ M^{-1}$.

It can be seen that the real experimental curves do not include clear linear domain. The lack of linear domain may suggest that the values of association constants of ClTPB$^-$ sites and K^+, Na^+, Cs^+, and NH_4^+ cations are low. Additional reason for the absence of linear domain in the emf curve is that these association constants are similar to K_{SR}—the association constant of TDDA$^+$ ClTPB$^-$ ion pairs. Processing of the results was, therefore, accomplished in two steps. First, data related to 2 experimental points (in each of the respective curve) producing linear response close to Nernstian have been treated with Eq. (12) giving initial values of K_{IR}. Next, these values were used for further fitting of the experimental curves. In this way, estimates of association constants of ion pairs formed by ClTPB$^-$ and K^+, Na^+, Cs^+, and NH_4, and also that of TDDA$^+$ ClTPB$^-$ ion pairs were obtained, for real membranes plasticized with BBPA and with oNPOE.

The estimated values of the association constants of ClTPB$^-$ ion pairs in membranes plasticized with BBPA are as follows: $K_{KClTPB} = 2.5 \times 10^3\ M^{-1}$, $K_{NaClTPB} = 2.0 \times 10^3\ M^{-1}$, $K_{CsClTPB} = 4.0 \times 10^3\ M^{-1}$, $K_{NH4ClTPB} = 3.2 \times 10^3\ M^{-1}$. Satisfactorily agreement between experimental and calculated curves is achieved with the same value of $K_{TDDAClTPB} = 2.5 \times 10^2\ M^{-1}$. The data measured for K^+ in oNPOE can be fitted with $K_{KClTPB} = 1.6 \times 10^3\ M^{-1}$, $K_{TDDAClTPB} = 10\ M^{-1}$. The number of the experimental points in each of the curves is small, and therefore, the accuracy of the estimated values cannot be high. However, calculations with values 2 times higher or 2 times lower than our estimates produce curves which significantly deviate from the experimental points, as illustrated in Fig. 4A for K^+. Therefore, we believe that the relative error of the estimated association constants is within ±100%, or within ±0.3 in logs, except of oNPOE where it is higher. It is known that the selectivity of membranes based on KClTPB with various plasticizers is low, i.e., selectivity coefficients to any of these ions over the rest are within ±1 (in logs). Therefore, one should not expect neither high, nor very different association constants for ion pairs formed by ClTPB$^-$ and K^+, Na^+, Cs^+, and NH_4^+ cations. Thus, the obtained results are consistent with what one could expect for tetraphenylborates.

4.2. Membranes containing Calcium bis[4-(1,1,3,3-tetramethylbutyl)phenyl]phosphate

Ion-pairing between Ca^{2+} and bis[4-(1,1,3,3-tetramethylbutyl)phenyl]phosphate (TMBPP$^-$) monovalent anion was studied in membranes plasticized with bis(dioctylphenyl)phosphonate. The latter plasticizer is commonly used in combination with TMBPP$^-$ and other alkylphosphoric cation exchangers [15,16]. The concentration of $CaTMBPP_2$ was the same in all the membranes: 2×10^{-2} m, giving 4×10^{-2} m for total concentration of the TMBPP. The cationic additive was TDA$^+$ which was added as TDABr, and the content of the additive was varied from 0 to 0.036 m, thus up to 90% (molar) relative to the main sites.

Electrodes with the membranes of all compositions showed near-Nernstian slope of 29.5 mV in $CaCl_2$ solutions within the range 10^{-5} to 10^{-1} M. Segmented sandwich membrane potentials measured with these compositions are presented in Fig. 6.

The experimental curve contains clearly resolved linear domain with the slope of 32.9 mV which is close to Nernstian value for divalent cations. Therefore, the sought association constant K_{CaR2} can be obtained directly by the use of Eq. (15), giving $K_{CaRR} \approx 1.6 \times 10^4\ M^{-1}$ ($\log K_{CaRR} \approx 4.2$). This constant is, however, the second step constant, $K_{CaRR} = \beta_{CaRR}/K_{CaR}$, while the first step constant is probably even higher. This must be the reason why the experimental curve indeed includes Nernstian linear domain, like the idealized theoretical curves shown in Fig. 3A.

For comparison of the value obtained potentiometrically using the novel version of the segmented sandwich method, calcium-selective membranes were studied also by chronopotentiometry. These membranes did not contain TDABr, while the concentration of $CaTMBPP_2$ was varied from 0.0021 to 0.021 m.

The respective curves are presented in Fig. 7A and B. One can see that the chronopotentiometric response is strongly dependent on the concentration of $CaTMBPP_2$ in membranes (Fig. 7A), while variation of the composition of solution for the same membrane produces virtually no change in the chronopotentiometric curve. This result suggests that the polarization is confined to membrane phase. On the other hand, the curves became linear if plotted against square root of time, suggesting diffusional nature of the polarization.

It is realistic to assume that monovalent ions CaTMBPP$^+$ and TMBPP$^-$ are strongly predominating over divalent free Ca^{2+} in the membranes. Since TMBPP$^-$ anion is rather bulky, the size of the two monovalent ions should be about the same, and therefore, also the mobilities of the species must be roughly the same. For such a situation, it was shown elsewhere [19] that diffusion coefficients and concentration of dissociated ions can be estimated separately if ρ bulk resistivity and η diffusion polarization are measured for the same membrane. The idea exploited in [19] was that $\rho \sim (CD)^{-1}$, while $d\eta/dt^{1/2} \sim C^{-1}D^{-1/2}$, where C stands for the concentration of dissociated ions, D stands for their diffusion coefficients, and t stands for time. The measured polarization is a sum of polarizations on each side of the membrane. In symmetric system where both sides of the membrane are of the same area and in contact with the same solution, polarizations on each side of the membrane are the same. Finally, concentration of dissociated electrolyte and diffusion coefficients of the respective ions can be described as below [19]:

$$C = \frac{32RT}{\pi F^2}\rho i^2 \left(\frac{d\eta}{dt}\right)^{-2} \quad (16)$$

$$D = \frac{\pi}{64}\rho^{-2} i^{-2} \left(\frac{d\eta}{dt}\right)^{2} \quad (17)$$

Here i stands for the density of the polarizing current. The results obtained are $\log D = -7.7 \pm 0.5$ and $\log K_{CaRR} = 4.8 \pm 0.7$. This estimate of the diffusion coefficient is consistent with values known from the literature [10,11,19,22,31,32]. The estimate of the association constant made by segmented sandwich membrane method: $\log K_{CaRR} \approx 4.2$ is in satisfactorily agreement with the value obtained by chronopotentiometric measurements.

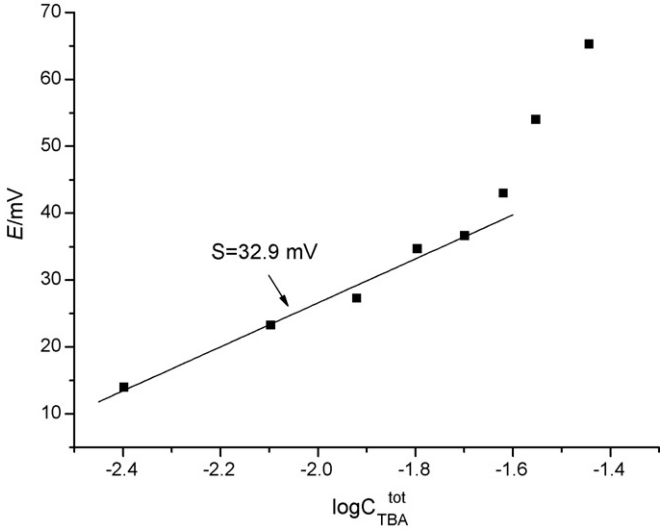

Fig. 6. Potentials of segmented sandwich membranes with $CaTMBPP_2$ and TDABr additive.

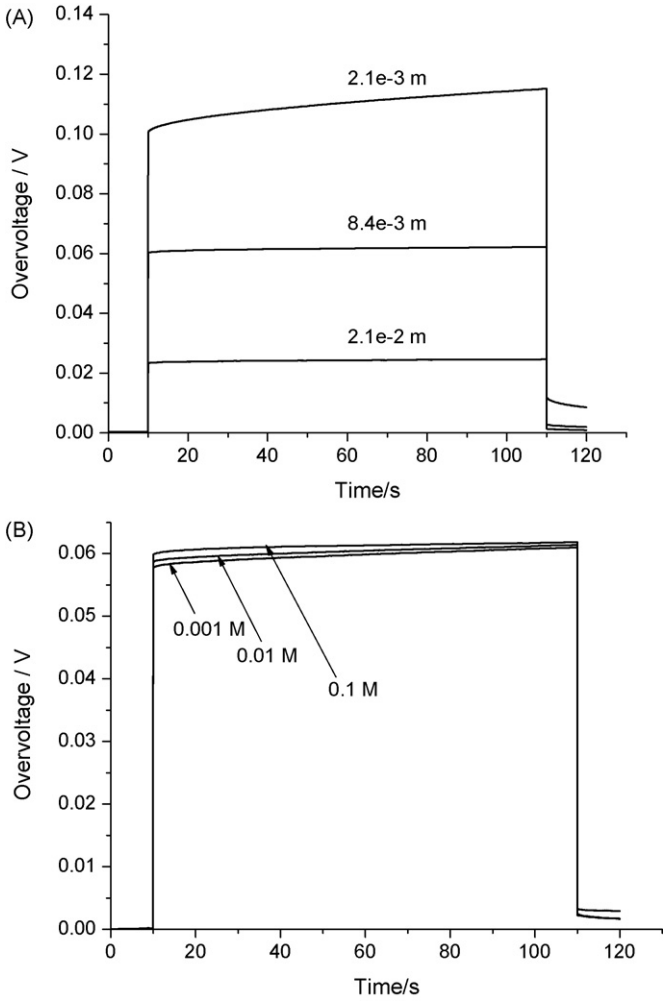

Fig. 7. Chronopotentiometric curves of membranes with different concentrations of $CaTMBPP_2$ in 0.1 M $CaCl_2$ (A), and of the membrane with 0.084 m $CaTMBPP_2$ in $CaCl_2$ solutions with different concentrations (B).

5. Conclusions

Segmented sandwich membrane method is a powerful tool which allows for better insight and characterization of species interactions in real ion-selective membranes. This paper demonstrates how the method can be modified for measuring ion-site association. The data obtained for the ion pairs of monovalent cations with tetra-*p*-Cl-phenylborate anion are consistent with the selectivity of their potentiometric response. Lower association constants in oNPOE as compared with those in BBPA are consistent with the polarity of the respective membranes. The estimated association constant of KClTPB in oNPOE: $K_{KClTPB} \approx 1.6 \times 10^3\ M^{-1}$ suggests that the association degree (when the total concentration is 0.01 M) is approximately 80%. Thus, even membranes plasticized with oNPOE cannot be considered fully dissociated.

Chronopotentiometric data obtained with calcium-selective membrane confirm the results of segmented sandwich membrane measurements.

In principal, the proposed technique may be useful for characterization of ion association in any organic solution immiscible with water, not only in ion-selective membranes, giving broader impact to electrochemistry.

On the other hand, the informative domain of the segmented sandwich potential curve belongs to relatively low concentrations of the ionic additive, and what is even more important—to low values of the registered EMF. Therefore, it is more demanding in relation to the accuracy of the data, and also the interpretation of the data is more complicated than in the case of complexation of ions by a neutral ionophore. The proposed method is also limited in relation to the value of association constant: the sensitivity of the signal to the association constant is lost if the latter is too high. As to the application of the method for measurements with divalent ions, it is at this point unclear how to access the first step, and also the cumulative association constant.

Acknowledgments

The authors greatly acknowledge Radiometer (Copenhagen), and personally Dr. Birgit Zachau-Christiansen for providing high purity ion-exchanger and plasticizer for calcium membranes.

References

[1] E. Bakker, Anal. Chem. 74 (2004) 3285.
[2] E. Bakker, Yu Qin, Anal. Chem. 78 (2006) 3965.
[3] E. Bakker, Analyt. Chem. 69 (1997) 1061.
[4] T. Sokalski, A. Ceresa, T. Zwickl, E. Pretsch, J. Amer. Chem. Soc. 119 (1997) 11347.
[5] R. Bereczki, B. Taka, J. Langmaier, M. Neely, R. Gyurcsanyi, K. Toth, G. Nagy, E. Lindner, Anal. Chem. 78 (2006) 942.
[6] W.E. Morf, M. Badertscher, T. Zwickl, N.F. de Rooij, E. Pretsch, J. Phys. Chem. B 103 (1999) 11346.
[7] T. Sokalski, A. Lewenstam, Electrochem. Commun. 3 (2001) 107.
[8] T. Sokalski, P. Lingenfelter, A. Lewenstam, J. Phys. Chem. 107 (2003) 2443.
[9] P. Lingenfelter, I. Bedlechowicz-Sliwakowska, T. Sokalski, M. Maj-Zurawska, A. Lewenstam, Anal. Chem. 78 (2006) 6783.
[10] W.E. Morf, The Principles of Ion-Selective Electrodes and of Membrane Transport, Akademiai Kiado, Budapest, 1981.
[11] E. Bakker, P. Bühlmann, E. Pretsch, Chem. Rev. 97 (1997) 3083.
[12] J. Sandblom, G. Eisenman, J.L. Walker, J. Phys. Chem. 71 (1967) 3862.
[13] E. Bakker, E. Malinowska, R.D. Schiller, M.E. Meyerhoff, Talanta 41 (1994) 881.
[14] U. Shaller, E. Bakker, U.E. Spichiger, E. Pretsch, Analyt. Chem. 66 (1994) 391.
[15] G.J. Moody, R.B. Oke, J.D.R. Thomas, Analyst 95 (1970) 910.
[16] A. Craggs, G.J. Moody, J.D.R. Thomas, Analyst 104 (1979) 412.
[17] P. Bühlmann, E. Pretsch, E. Bakker, Chem. Rev. 98 (1998) 1593.
[18] K.N. Mikhelson, Electroanalysis 15 (2003) 1236.
[19] K.N. Mikhelson, V.M. Lutov, K. Sulko, O.K. Stefanova, Sov. Electrochem. 24 (1988) 1369, Russ., Engl. transl.
[20] S.B. Mokrov, O.K. Stefanova, E.A. Materova, E.E. Ivanova, Vestn. Leningr. Univ. 16 (1984) 41, In Russian.
[21] K.N. Mikhelson, Sens. Actuators B 18 (1994) 31.
[22] V.M. Lutov, K.N. Mikhelson, Sens. Actuators B 19 (1994) 400.
[23] Y. Mi, E. Bakker, Anal. Chem. 71 (1999) 5279.
[24] Y. Qin, Y. Mi, E. Bakker, Anal. Chim. Acta 421 (2000) 207.
[25] M.M. Shultz, O.K. Stefanova, S.B. Mokrov, K.N. Mikhelson, Anal. Chem. 74 (2002) 510.
[26] K.N. Mikhelson, J. Bobacka, A. Ivaska, A. Lewenstam, M. Bochenska, Anal. Chem. 74 (2002) 518.
[27] K.N. Mikhelson, A. Lewenstam, Sens. Actuators B 48 (1998) 344.
[28] K.N. Mikhelson, A. Lewenstam, S.E. Didina, Electroanalysis 11 (1999) 793.
[29] K.N. Mikhelson, A. Lewenstam, Anal. Chem. 72 (2000) 4965.
[30] Y. Qin, E. Bakker, Anal. Chem. 74 (2002) 3134.
[31] U. Oesch, W. Simon, Helv. Chim. Acta 62 (1979) 754.
[32] P. Bühlmann, Y. Umezawa, S. Rondinini, A. Vertova, A. Pigliucci, L. Bertesago, Anal. Chem. 72 (2000) 1843.